

# Evaluation of the Resistance and Bioactivity of Wollastonite and Hydroxyapatite Coated Zirconia Dental Implant Material

## Wollastonite ve Hidroksiapatit Kaplı Zirkonya İmplant Materyalinin Bağlantı Dayanıklılığı ve Biyoaktivitesinin Değerlendirilmesi

Şefik KOLÇAKOĞLU<sup>a</sup>, Anıl ÖZYURT<sup>b</sup>, Fatih ÜSTEL<sup>c</sup>

<sup>a</sup>Nimet Bayraktar Dental Clinic, Kayseri, TURKEY

<sup>b</sup>Trakya University Faculty of Dentistry, Department of Oral and Maxillofacial Surgery, Trakya, TURKEY

<sup>c</sup>Sakarya University Faculty of Engineering, Department of Metallurgical and Materials Engineering, Sakarya, TURKEY

**ABSTRACT Objective:** Zirconia dental implants are an alternative to titanium. Various studies have been carried out in order to improve the surface properties of zirconia implants like titanium implants. The aim of this study is to evaluate the resistance and bioactivity of zirconia dental implant materials coated with different ratios of hydroxyapatite and wollastonite powders by plasma spray method. **Material and Methods:** The bond strength between the zirconia and the coatings was measured according to the ASTM C-633 standard. The data were obtained by using one-way analysis of variance. Differences between the groups were determined by Post Hoc Tukey HSD test. Examples prepared for bioactivity testing were kept in 37 °C simulated body fluid for 2, 7, 14- and 21-day periods. Changes in the sample surfaces were analyzed by scanning electron microscopy using energy distribution x-ray spectrometry and x-ray diffraction device. **Result:** Bonding values of coatings containing different ratios of W were found to be significantly higher than pure HA coatings ( $p < 0.05$ ). **Conclusion:** All sample groups used in the study showed bioactive properties in simulated body fluid.

**Keywords:** Zirconia implant; plasma spray; wollastonite; hydroxyapatite; bioactivity; simulated body fluid

**ÖZET Amaç:** Zirkonya, titanyuma alternatif olarak kullanılan dental implant materyalidir. Zirkonya implantların yüzey özelliklerinin geliştirilmesi için bir çok çalışma yapılmaktadır. Bu çalışmanın amacı farklı oranlarda wollastonit ve hidroksiapatitle kaplanmış zirkonyanın bağlantı dayanıklılığı ve biyoaktivitesini değerlendirmektir. **Gereç ve Yöntemler:** Zirkonya ve kaplama materyali arasındaki bağlantı dayanıklılığı ASTM C-633 standardına uyularak ölçüldü. Veriler tek yönlü varyans ile analiz edildi. Gruplar arası fark Post Hoc Tukey HSD testi ile saptandı. Kaplanmış örnekler 2, 7, 14 ve 21 günlük periyotlarla 37 derecedeki yapay vücut sıvısı içerisinde bekletildi. Örnek yüzeylerindeki değişimler, x-ışını spektrometre ve x-ışını difraksiyon ölçebilen taramalı elektron mikroskobu yardımıyla analiz edildi. **Bulgular:** Wollastonit içeren tüm gruplarda bağlantı dayanıklılığı ve biyoaktivite değerleri saf hidroksiapatit kaplı gruba kıyasla anlamlı olarak yüksek bulundu ( $p < 0.05$ ). **Sonuç:** Çalışmanın tüm örnek grupları yapay vücut sıvısı içerisinde bioaktif özellik göstermiştir.

**Anahtar Kelimeler:** Zirkonya implant; plazma sprey; wollastonit; hidroksiapatit; biyoaktivite; yapay vücut sıvısı

Zirconia is used as a dental implant material due to its high resistance, biocompatibility, and the success of osseointegration.<sup>1</sup> Nowadays, zirconia dental implants are used as an alternative to titanium alloy implants for their aesthetic and biochemical properties.<sup>2-5</sup>

The characteristic of the bone-contacting surface of the implant, as well as the raw material, directly affects the success of osseointegration.<sup>6</sup> Many phys-

ical and chemical methods facilitate implant surface preparation. Plasma spray coating method using biocompatible materials has recently become popular. This method supports the potential of osseointegration by allowing the implant to be coated with various biocompatible powders (ceramics, metals, etc.) to prevent oxidation, corrosion and to ensure heat resistance.<sup>7</sup>

**Correspondence:** Anıl ÖZYURT

Trakya University Faculty of Dentistry, Department of Oral and Maxillofacial Surgery, Trakya, TURKEY/TÜRKİYE

**E-mail:** anilozyurt@trakya.edu.tr



Peer review under responsibility of Türkiye Klinikleri Journal of Dental Sciences.

**Received:** 23 Nov 2019 **Accepted:** 19 Feb 2020 **Available online:** 24 Feb 2020

2146-8966 / Copyright © 2020 by Türkiye Klinikleri. This is an open access article under the CC BY-NC-ND license (<http://creativecommons.org/licenses/by-nc-nd/4.0/>).

The most commonly used materials for surface coating are the hydroxyapatite and calcium phosphate salts. Hydroxyapatite is a biocompatible ceramic substance having a chemical composition and crystal structure similar to apatite found in the human skeletal system. Although there are positive outcomes of osseointegration regarding the hydroxyapatite coating layers, studies have reported that there are problems such as release from the surface and decomposition.<sup>8</sup>

Wollastonite is a natural ceramic with calcium metasilicate structure. Studies have shown that wollastonite has a high bioactive potential and a wide range of use in biomedical applications.<sup>9-15</sup> Some researchers have noted that wollastonite is more bioactive than hydroxyapatite in simulated body fluid.<sup>9,16</sup> The aim of this study is *in-vitro* evaluation of the success of hydroxyapatite and wollastonite bioceramic materials on the surface of the zirconia dental implant. In our study, zirconia samples having similar content used in dentistry were coated by means of the plasma spray. Bond strength and bioactivity of the bioceramic coated samples were examined.

## MATERIALS AND METHODS

This study was conducted in Gazi University, Faculty of Dentistry and Sakarya University, Thermal Spray Research and Application Laboratory. Our study is an *in vitro* material experiment so there was no need to ethical approval.

In the study, semi-sintered yttria and stabilized tetragonal zirconia polycrystalline samples (Ice Zircon; Zirkozahn, Gais, Italy) were coated with the mixture of hydroxyapatite (HA) and wollastonite (W) powders in different proportions by using plasma spray method. We used fabricated products having chemical properties of certain standards called HA powder Captal® 30 S Hydroxylapatite (Plasma Biotall Ltd., Derbyshire, UK), W powder Calcium silicate, meta, Reagent Grade (Alfa Aesar GmbH & Co., Karlsruhe, Germany) for the coating.

### PREPARATION OF POWDER MIXTURES

Before the preparation of HA and W powder mixtures, the powders were dried in an oven (Nüve FN 500, Ankara, Turkey) at 75 °C for 1 hour. Four different coating materials were obtained according to the dif-

**TABLE 1:** Powder mixtures prepared and their abbreviated names.

Mixing Ratio	Abbrev.	Total
100% Hydroxyapatite	HA	300g
70% HA 30% Wollastonite	H7W3	210g HA + 90g W = 300g
30% HA 70% Wollastonite	H3W7	90g HA + 210g W = 300g
100% Wollastonite	W	300g

ferent mixing ratios by considering the studies performed with the W powder mixture as indicated in Table 1.<sup>13,17</sup>

H7W3 and H3W7 powder mixtures were stirred in a three-axis automatic mixer for one hour each to make them as homogeneous as possible (Turbula, Willy A. Bachofen AG Maschinenfabrik, Muttenz, Switzerland). Scanning electron microscope (SEM) images were also examined to observe the homogeneity of the mixtures at the microscopic level.

### PREPARATION OF ZIRCONIA SAMPLES

Samples in different geometric shapes for different researches were formed by CAD-CAM milling (Yenamak D40, İstanbul, Turkey) from the blocks in the structure of tetragonal zirconia polycrystalline stabilized with semi-sintered yttria (YTZP). In order to measure the bonding values, 20-cylinder samples with 25.4 mm diameter and 10 mm height were prepared in compliance with ASTM C633.<sup>18</sup> standard; for bioactivity test, 40 pieces of square prism samples with 10 mm x 10 mm x 5 mm dimensions were prepared (Figure 1). All samples obtained by milling

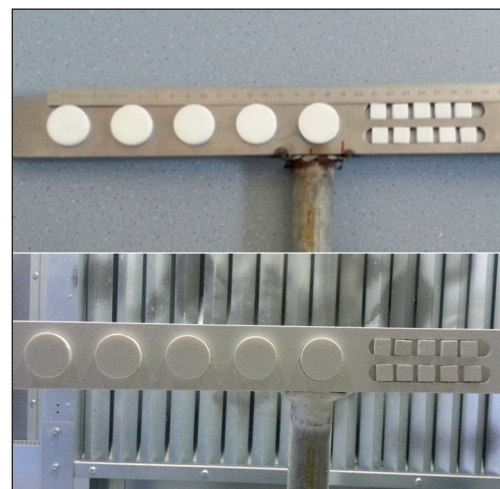


**FIGURE 1:** The image of zirconia samples before and after coating.

were subjected to the sintering process at 1500 °C by gradually heating in an oven (Tegra MP1500, İstanbul, Turkey) for 10 hours.

### PLASMA SPRAY COATING PROCESS

Sintered sample surfaces were sandblasted with 3 atm pressure for 20 seconds at a distance of 120 mm from a 90° angle with Al<sub>2</sub>O<sub>3</sub> powders (Sicheng, Henan, China) with the F60 particle size (250µm). Afterwards they were cleaned with high-pressure air and prepared for plasma spray process.<sup>13,19</sup>

The sandblasted samples were fixed with a metal holder and positioned perpendicular to the plasma spray flame at a 100 mm distance and the samples heated (Figure 2). After heating, the samples were separated into groups according to the coating type with HA, H7W3, H3W7 and W powders using the plasma spray parameters specified in Table 2 (F4-MB, Sulzer Metco, Basel, Switzerland).

### EXAMINATION OF PLASMA SPRAY COATINGS USING SCANNING ELECTRON MICROSCOPE

Sample surfaces and sections of the samples were examined with SEM (Tegrapol-21, Struers, Denmark) to analyze the microstructure of the coatings.<sup>20</sup>

### MEASURING BONDING STRENGTH AND STATISTICS

Resistance testing according to the ASTM C-633 standard was applied to measure the bond strength between the coating material and the zirconia surface (Z050, Zwick Roell, Ulm, Germany). The tensile force with the speed of 0.013 mm/sec - 0.021 mm/sec was applied to the specimens prepared for the test until a rupture was observed. The bonding strength value (MPa) at the time of rupture was calculated by dividing the highest applied force (N) to the bonding surface area (mm<sup>2</sup>).

Data obtained from the groups were evaluated using one-way analysis of variance (ANOVA) (Minitab16, Minitab Incorporation, Pennsylvania, U.S.A). Differences between the groups were examined by the method of Post Hoc Tukey HSD.

### EVALUATION OF BIOACTIVITY OF SAMPLES

Simulated body fluid (SBF) having 35-38°C with pH values between 7.40-7.45 was prepared using the com-

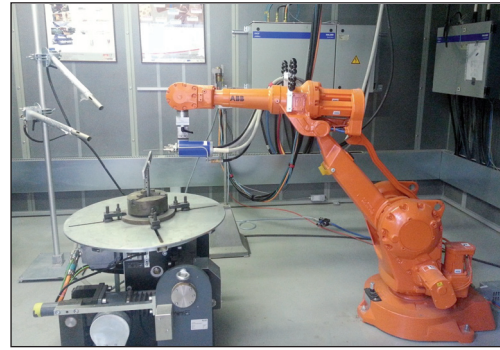


FIGURE 2: Plasma spray device used in coating process.

TABLE 2: Plasma spray parameters.

Argon	60 nlpm
Hydrogen	10 nlpm
Hydrogen (Carrier gas)	3,5 nlpm
Disk speed	18,5%
Scan speed (coating)	300mm/sec
Scanning speed (heating)	500mm/sec
Voltage	68V
Ampere	600A
Airjet	3 bar
Distance	100 mm

ponents specified in Table 3 in order to evaluate the bioactivities of the samples coated with bioceramics.<sup>21</sup>

Plasma spray coated samples were kept in an acetone bath using ultrasonic cleaner (Sonorex, Bandelin Electronic GmbH & Co., Berlin, Germany) before being placed in the SBF.<sup>11,22</sup> The samples were rinsed with distilled water after the acetone bath and dried at room temperature. Following the SBF for bioactivity test, samples were kept in the oven at 37°C (Nüve FN 400, Ankara, Turkey) for 2, 7, 14 and 21-day periods.<sup>11,23</sup> The SBF solutions used during the experiment period were renewed every other day. Following the incubation period, the samples were rinsed with distilled water and dried at room temperature. Afterwards, they were examined by scanning electron microscope-energy dispersive spectroscopy (SEM-EDS) and X-Ray Diffraction (XRD) methods.

### SURFACE ANALYSIS OF SAMPLES

#### *SEM-EDS Analysis*

After the bioactivity test was completed on the samples coated with gold, an EDS connected SEM

**TABLE 3:** Compounds used in simulated body fluid preparation.

Compound	Qty. (g)	Purity %	Formula weight	
1 NaCl	8.039	99.5	58.4430	(Merck,6400,Germany)
2 NaHCO <sub>3</sub>	0.355	99.5	84.0068	(Merck,6323,Germany)
3 KCl	0.225	99.5	74.5515	(Merck,4935,Germany)
4 K <sub>2</sub> HPO <sub>4</sub> - 3H <sub>2</sub> O	0.231	99.0	228.2220	(Merck,5099,Germany)
5 MgCl <sub>2</sub> - 6 H <sub>2</sub> O	0.311	98.0	203.3034	(Merck,5833,Germany)
6 1.0 M - HCl	39 ml			(Merck, 314, Germany)
7 CaCl <sub>2</sub>	0.292	95.0	110.9848	(Merck,2387,Germany)
8 Na <sub>2</sub> SO <sub>4</sub>	0.072	99.0	142.0428	(Merck,134462,Germany)
9 Tris(hydroxymethyl)aminomethane H <sub>2</sub> NC(CH <sub>2</sub> OH) <sub>3</sub>	6.118	99.0	121.1358	(Merck,8387,Germany)
10 1.0 M - HCl	0-5 ml			(Merck,314, Germany)

(Vega II, Tescan, PA, USA) device was used to examine the changes on the surface. While the microstructures of the sample surface were examined with SEM at an alternating voltage of 20 kV, the chemical analyzes of the particles on the surface were performed with EDS.

#### *XRD Analysis*

Surface analyzes of the samples were performed with XRD apparatus using a monochromatic CuK  $\alpha$  beam (40kV, 36 mA) (D/Max 2200, Rigaku Co, Tokyo, Japan). Sample surfaces were scanned with 2°/min between the angles of 20: 10°-90° and their density values were recorded graphically.<sup>24</sup>

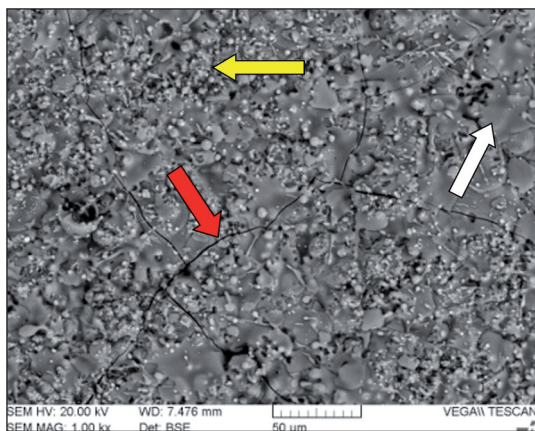


**FIGURE 3:** The SEM image taken at 1000x magnification of the HA-coated sample surfaces. The white arrow indicates the fully melted particle. The yellow arrow indicates the partially-melted particles. The red arrow indicates micro-cracks.

## RESULTS

### SURFACE SEM IMAGES OF PLASMA SPRAY COATINGS

Fully melted and partially-melted particles can be seen on the sample surface coated with HA. Micro-cracks are observed on the surface (Figure 3).

In the sample surface covered with H7W3 powder, fully melted, partially-melted and non-melted pieces are observed. Micro-crack formation is observed less than HA group (Figure 4).

On the surface of the samples coated with H3W7 powder, fully melted particles are observed to be more intense than the partially and non-melted

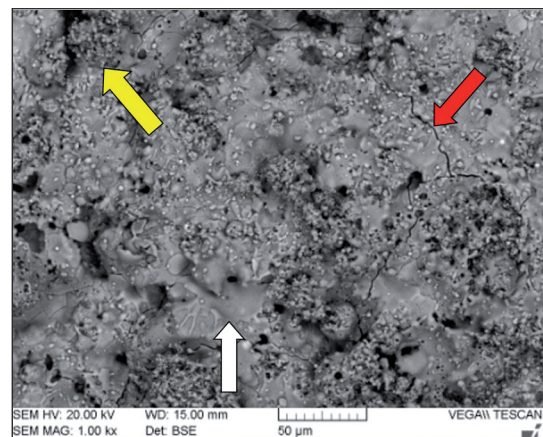


**FIGURE 4:** The SEM image taken at 1000x magnification of the H7W3-coated sample surfaces. The white arrow indicates the fully melted particle. The yellow arrow indicates the partially-melted particles. The red arrow indicates micro-cracks.

particles. Microfractures are seen throughout the surface (Figure 5). There are fully and partially-melted particles found on the sample surfaces covered with W powder. A small amount of micro-crack formation is observed on the sample surface (Figure 6).

### SECTIONAL SEM IMAGES OF PLASMA SPRAY COATED SAMPLES

The contact surface between the coating and zirconia and the coating layers is clearly seen on the sections taken (Figure 7).

In the cross-sectional examination of the HA coating, microcracks were observed in the coating layer horizontally and vertically. The HA coating was in lamellae structure and contains porosity. In the SEM images, significant separations were found in the HA coating-zirconia interface bond area compared to the other groups.

In the H7W3 coating section, it was observed that the coating consisting of hydroxyapatite and wollastonite powders exhibited lamellas structure and contained some porosity.

A small amount of horizontal and vertical microcracks were identified in the examined areas. No separation was found in the interface bond zone.

In the cross-sectional examination of the H3W7 coating, lamella structure consisting of wollastonite and hydroxyapatite powders can be observed. A small number of microcracks and porosity in the structure was observed.

In the W coating section analysis, it is possible to state a dense coating with less porosity compared to the other groups. A small amount of micro-crack is observed in the coating layer; W coating and zirconia bonding area show continuity.

### BOND STRENGTH VALUES AND STATISTICS OF PLASMA SPRAY COATINGS

The surface images and bond strength values of the samples subjected to ASTM C-633 standard resistance tests are shown in Figure 8.

Average bond strength values, standard deviation values, lowest and highest bond strength values obtained from each of the sample groups are given in Table 4. As a result of one-way analysis of variance, the p-value was determined as 0.005 which indicated

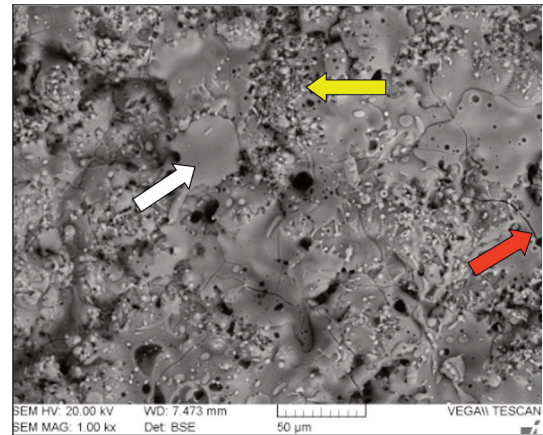


**FIGURE 5:** The SEM image taken at 1000x magnification of the H3W7-coated sample surfaces. The white arrow indicates the fully melted particle. The yellow arrow indicates the partially-melted particles. The red arrow indicates micro-cracks.

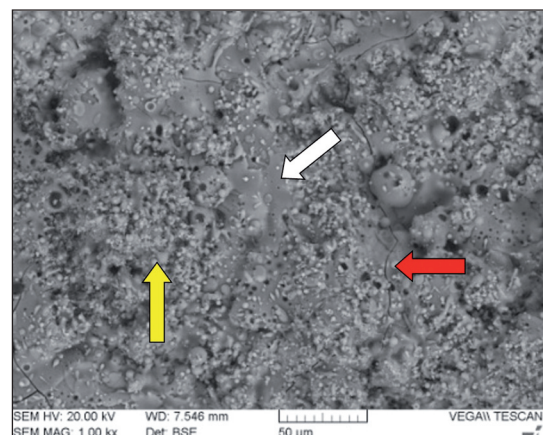


**FIGURE 6:** The SEM image taken at 1000x magnification of the W-coated sample surfaces. The white arrow indicates the fully melted particle. The yellow arrow indicates the partially-melted particles. The red arrow indicates micro-cracks.

a statistical difference between the groups ( $p < 0.05$ ). After the statistical analysis, there was no statistically significant difference found between the mean bond values of H7W3, H3W7 and W groups ( $p \geq 0.05$ ), whereas the bond strength of the HA group samples was significantly lower than the bond strength of other groups ( $p < 0.05$ ).

### EVALUATION OF BIOACTIVE PROPERTIES OF SAMPLES

#### *SEM Analyses*

Carbonhydroxyapatite (CHA) accumulation and microcracks were observed in all the coated surfaces of the samples which were kept for 2, 7, 14- and 21-days periods in the SBF. It has been noted that in-

creased incubation time in the SBF, increased the layer of CHA accumulated on the surface (Figure 9, Figure 10, Figure 11, Figure 12).

### EDS Analyses

According to the results of EDS analysis of the samples kept in SBF, a decrease in Ca and P amount

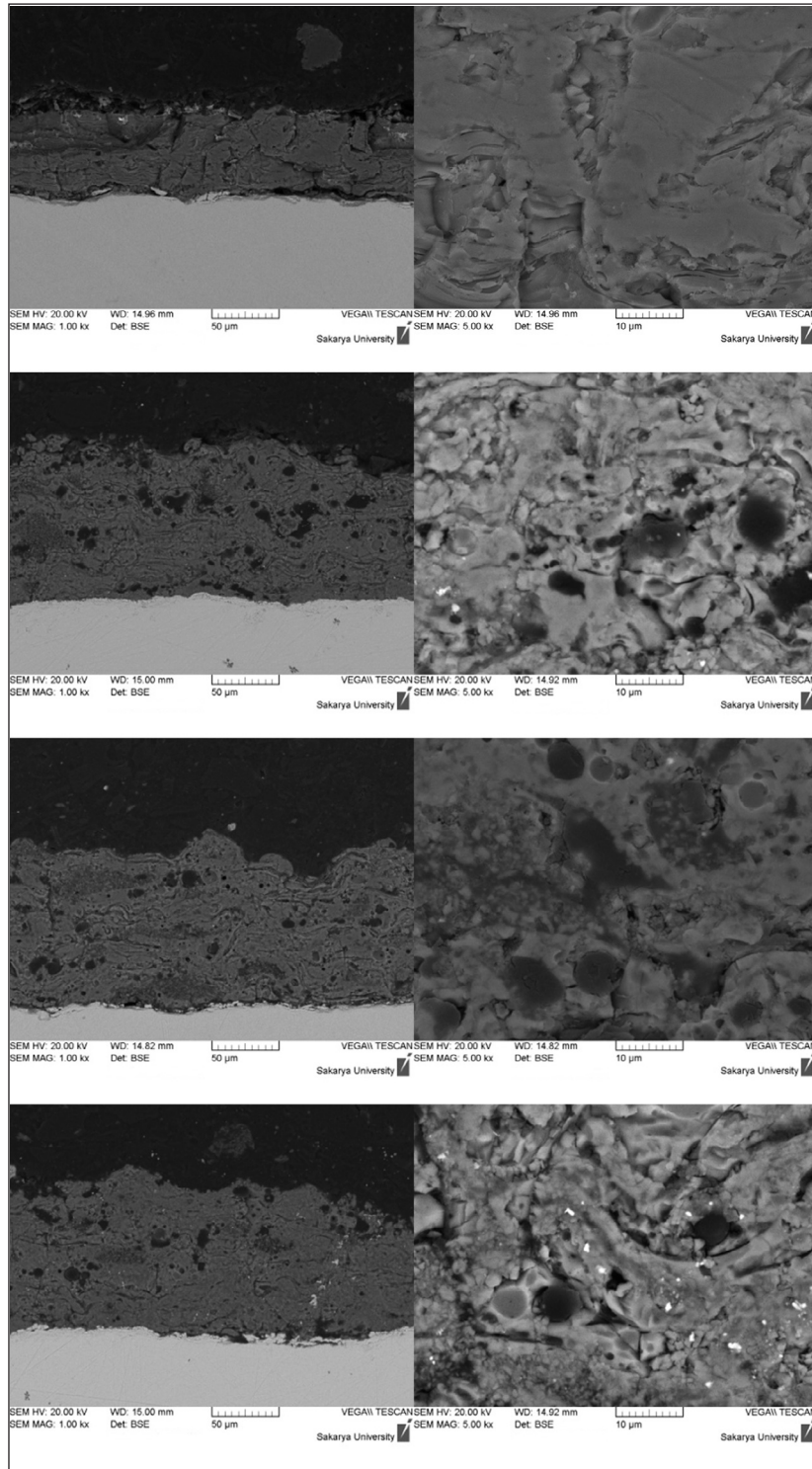


**FIGURE 7:** Samples of H, H7W3, H3W7 and W groups respectively from top to bottom; SEM images at 1000x and 5000x magnification respectively from left to right.

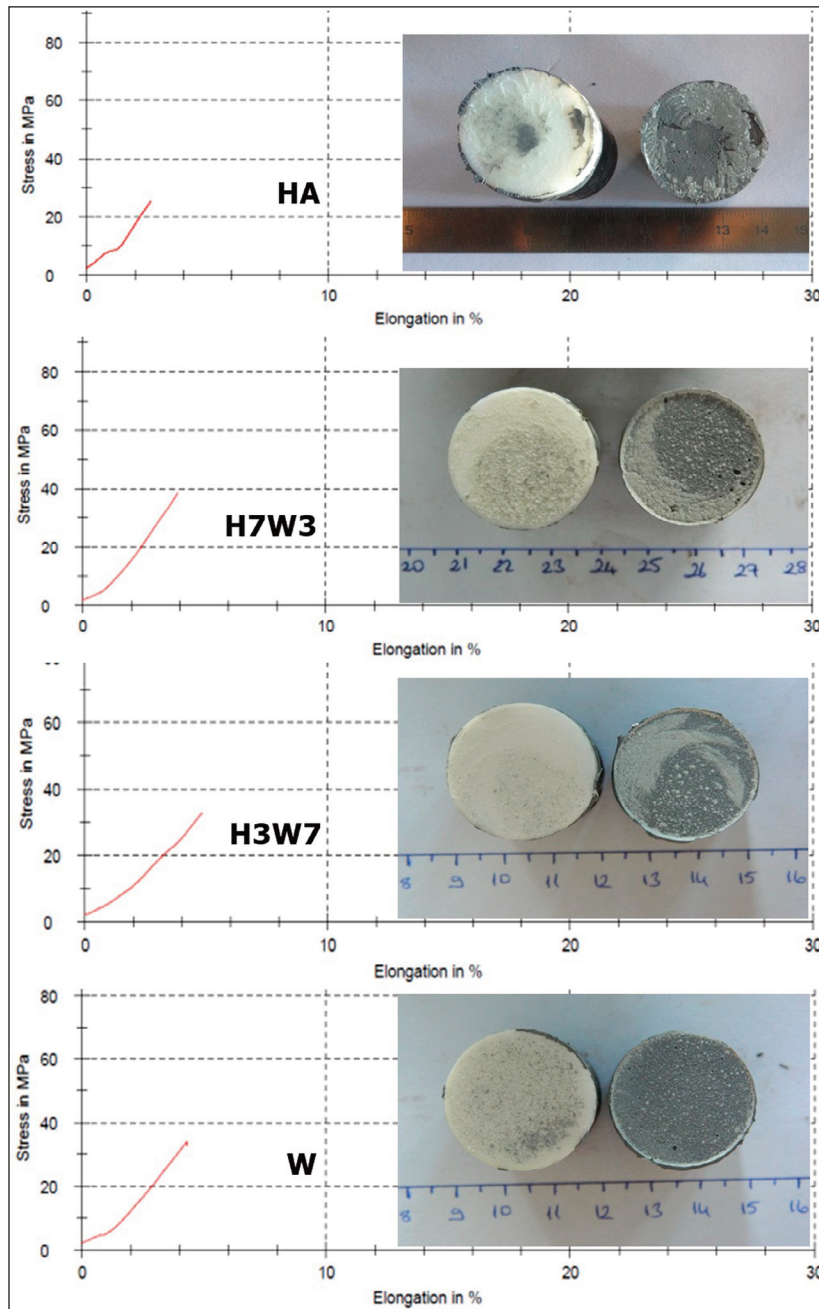
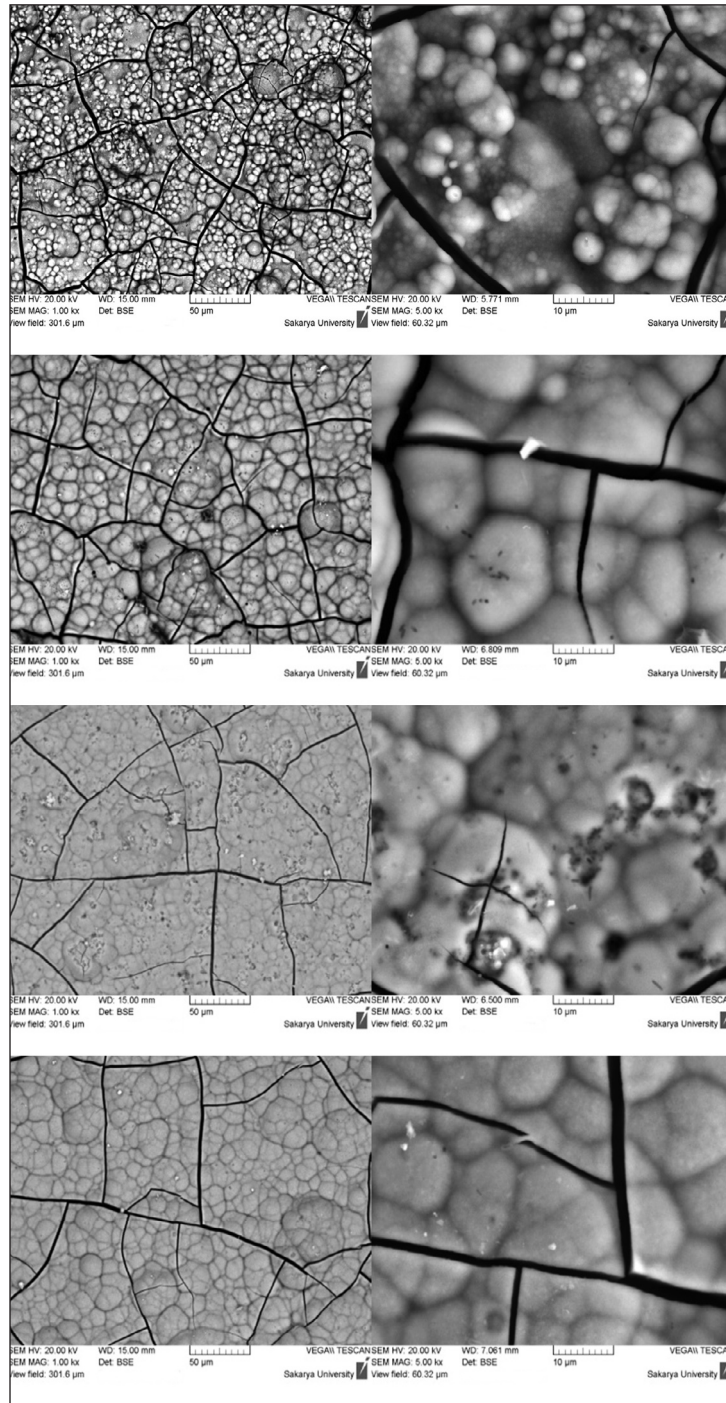


FIGURE 8: Surface images and bonding values of samples of HA, H7W3, H3W7 and W groups after tensile test from top to bottom respectively.

was observed in all groups as of the second day. The peak of the silicate which can be observed on the EDS analysis of the 2+ day for the H7W3, H3W7 and W groups containing wollastonite powder cannot be seen in the surface analysis of 7, 14 and 21-day samples (Graph 1, Graph 2, Graph 3, Graph 4).

**TABLE 4:** Statistical summary of bond strength values of sample group.

	N	Average MPa	Standard deviation	Lowest	Highest
HA	5	23	2,345	21	26
H7W3	5	31	5,523	24	38
H3W7	5	31	3,082	26	33
W	5	31,66	2,608	28	35



**FIGURE 9:** From top to down respectively, images of the HA group samples kept in SBF for 2, 7, 14 and 21 days; at 1000x and 5000x magnification respectively from left to right.

### *XRD Analyses*

The coated surfaces were examined by using an X-ray diffraction device to evaluate the bioactive properties of the sample groups HA, H7W3, H3W7 and W which were kept in SBF for 21 days.

To evaluate the XRD curves obtained, Tricalcium phosphate (TCP), hydroxyapatite (HA), calcium oxide (CaO), 2M-wollastonite (2M-W), CaSiO<sub>3</sub> (W) and zirconia (ZrO<sub>2</sub>) XRD reference cards were used. XRD curves of the groups are given in [Graph 5](#),



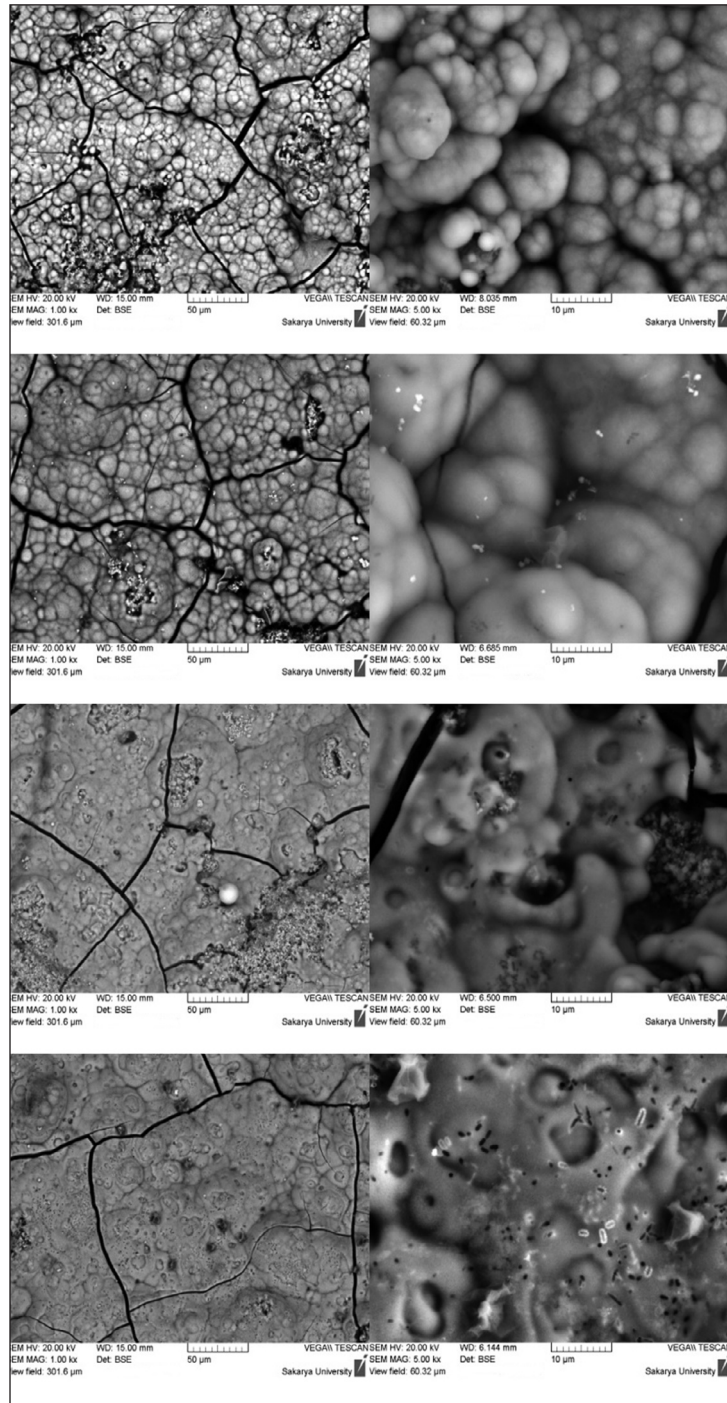


**FIGURE 10:** From top to down respectively, images of the H7W3 group samples kept in SBF for 2, 7, 14 and 21 days; at 1000x and 5000x magnification respectively from left to right.

[Graph 6](#), [Graph 7](#) and [Graph 8](#). The peaks obtained in XRD analyzes coincide with the characteristic peaks of hydroxyapatite. The XRD curves in the HA, H7W3, H3W7, and W groups are in consistency with

the standard diffraction pattern of hydroxyapatite (Card No: 09-0432). As a result of XRD analysis, it was concluded that the CHA layer was formed on the surfaces of HA, H7W3, H3W7 and W sample groups.

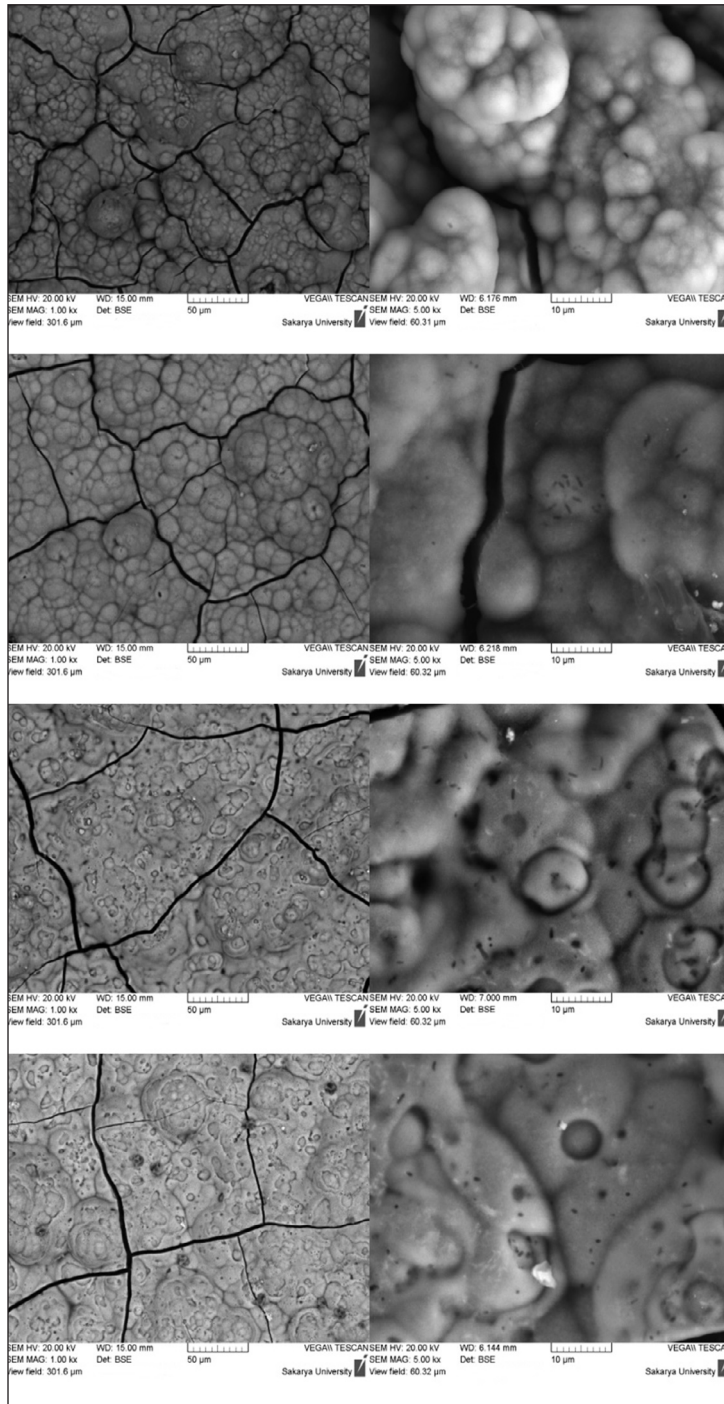


**FIGURE 11:** From top to down respectively, images of the H3W7 group samples kept in SBF for 2, 7, 14 and 21 days; at 1000x and 5000x magnification respectively from left to right.

## DISCUSSION

As in titanium alloy implants, zirconia dental implant surfaces were shaped by abrasion or coating in order to increase the bone implant bonding, to shorten the

healing time and to perform an earlier prosthetic loading.<sup>5,25-28</sup>

HA coatings, which are one of the coatings made on titanium implants, have various negative features such as poor bonding resistance, low crystal phase

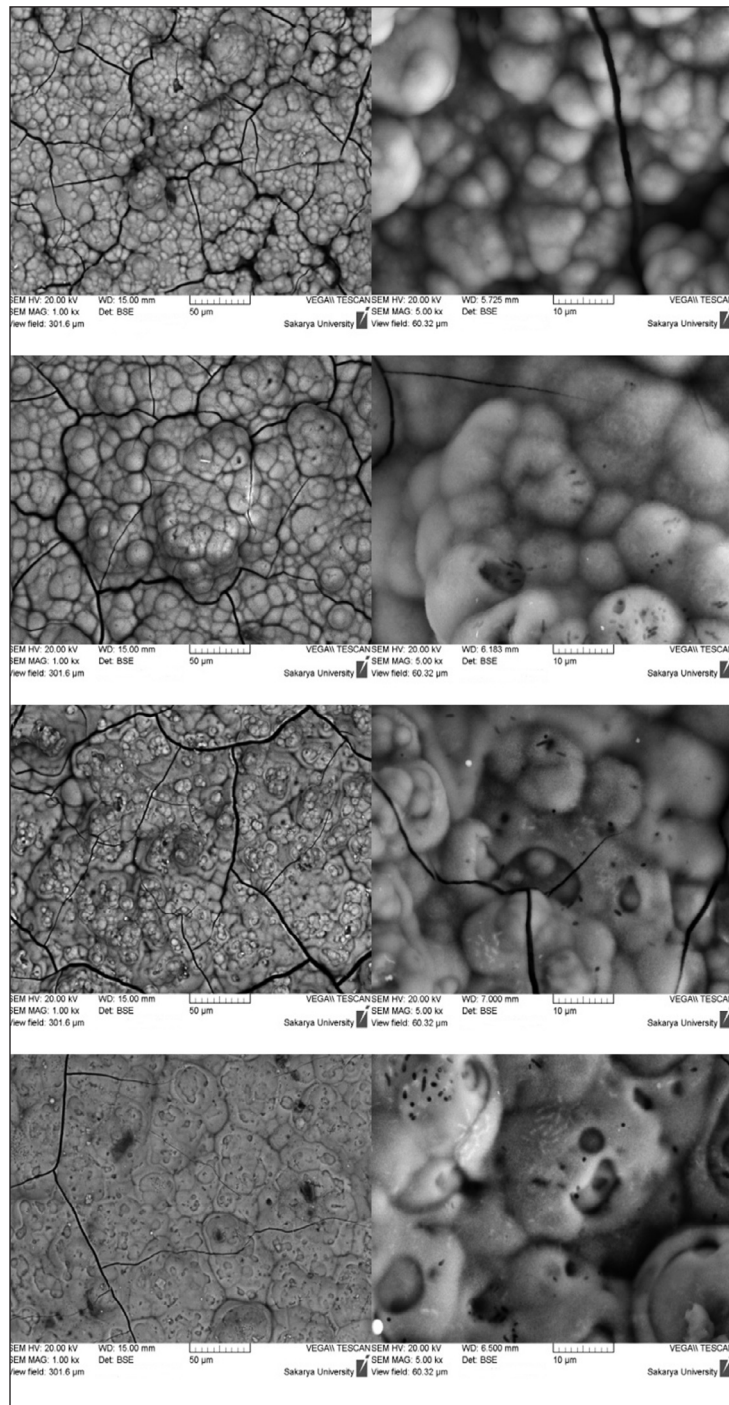
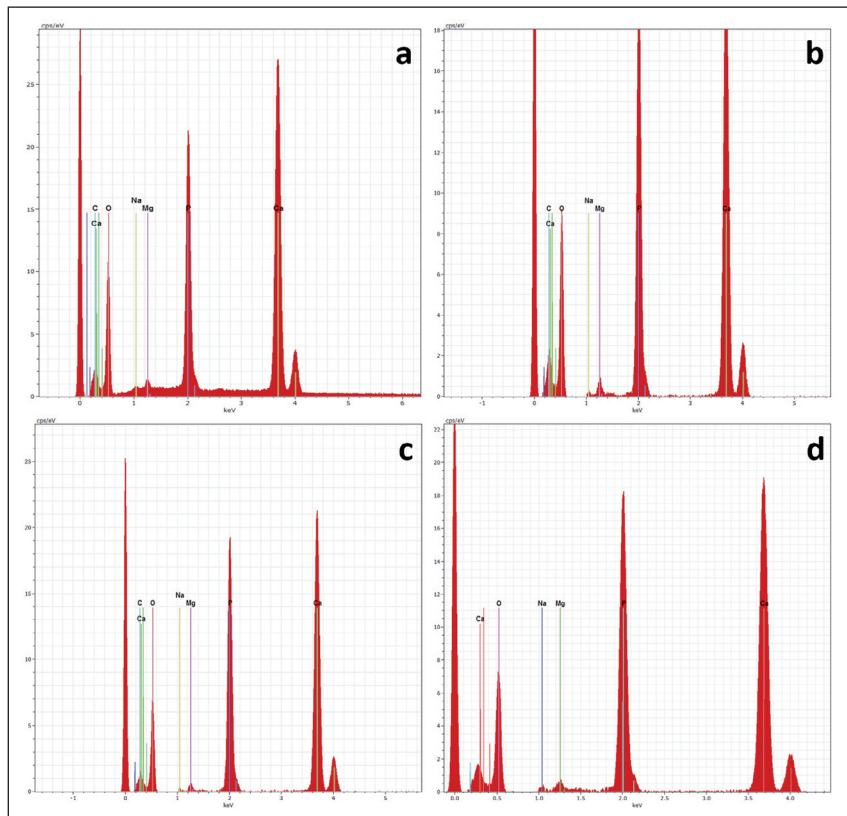


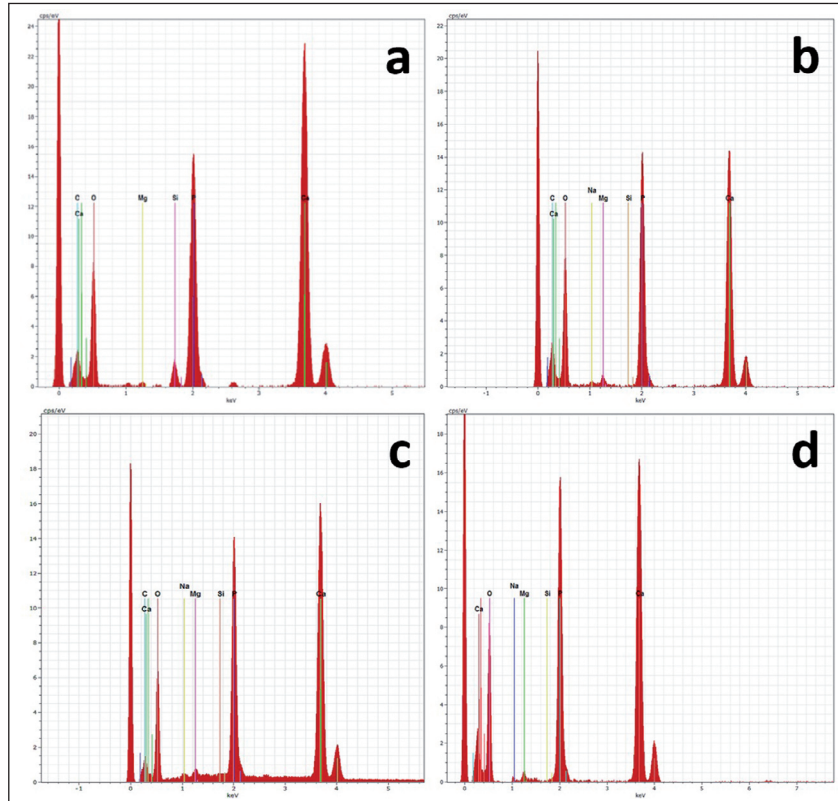
**FIGURE 12:** From top to down respectively, images of the W group samples kept in SBF for 2, 7, 14 and 21 days; at 1000x and 5000x magnification respectively from left to right.

ratio, phase change at high temperature during the plasma spray process and rupture of the coating surface in the body.<sup>8,9,29</sup> Therefore, some researchers have aimed to obtain a stronger and more stable coating by adding different metals/ceramics to the

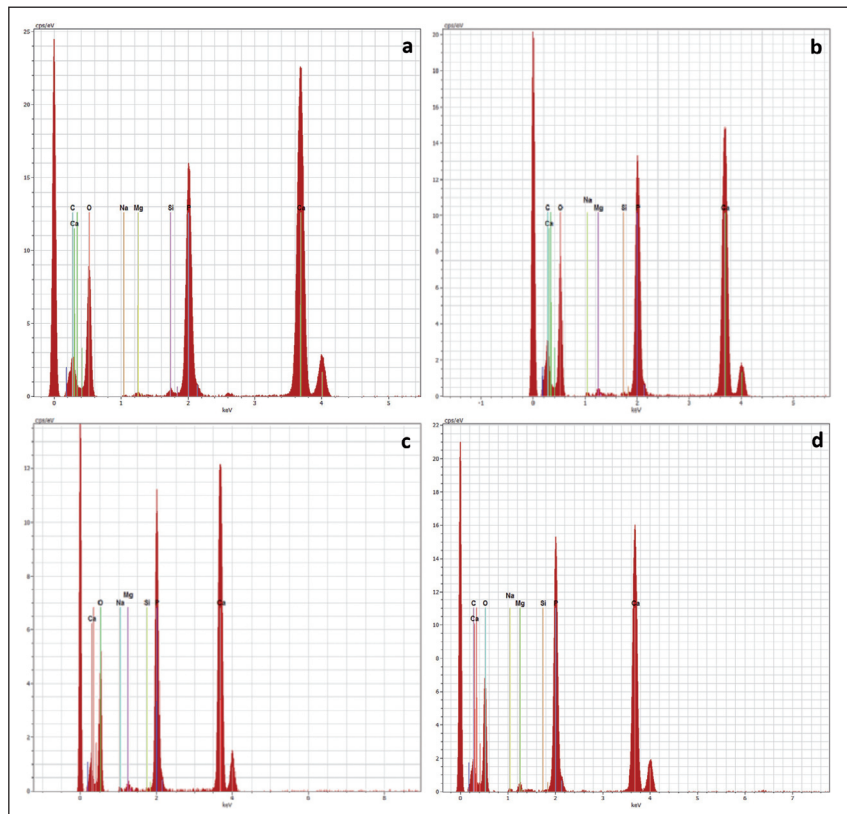
hydroxyapatite structure.<sup>24,29-31</sup> Recently, some studies have indicated that wollastonite (calcium silicate -  $\text{CaSiO}_3$ ) would be suitable as the coating material due to its bond strength and bioactive properties.<sup>8,10,11,32-34</sup>



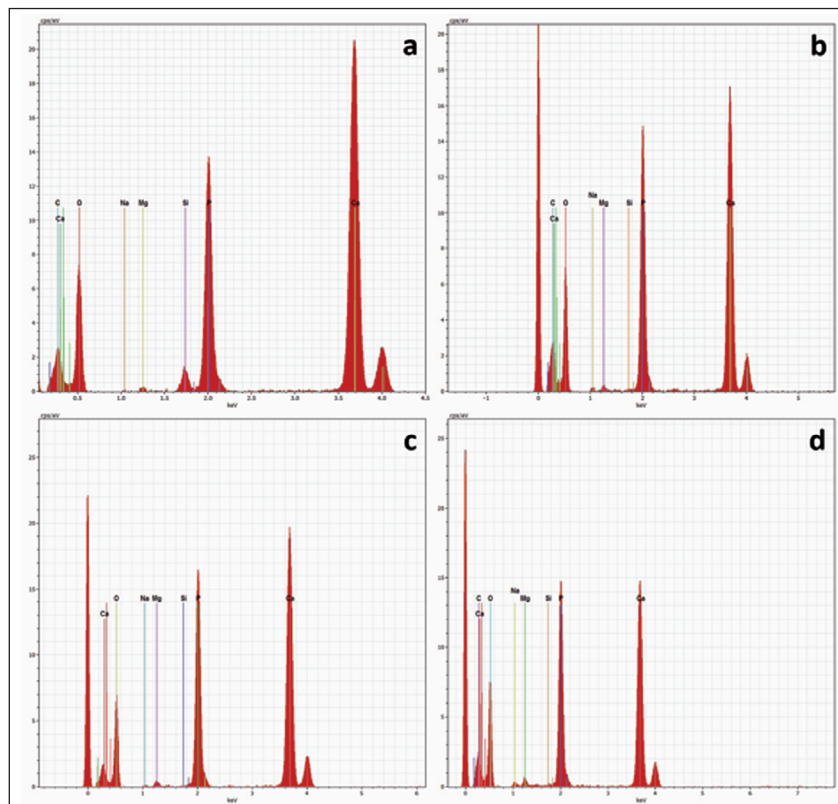
GRAPH 1: a) 2, b) 7, c) 14, d) 21-day EDS analysis of the HA group samples kept in SBF.



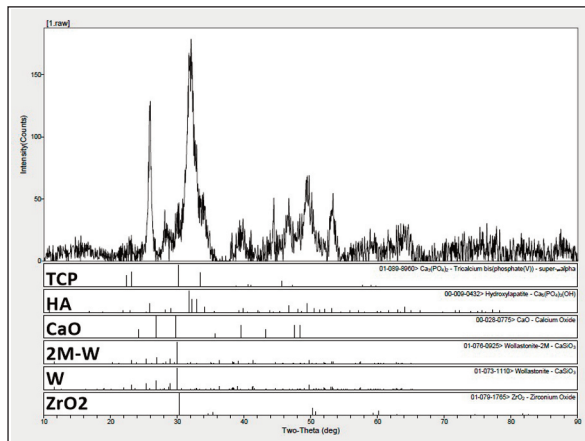
GRAPH 2: a) 2, b) 7, c) 14, d) 21-day EDS analysis of the H7W3 group samples kept in SBF.



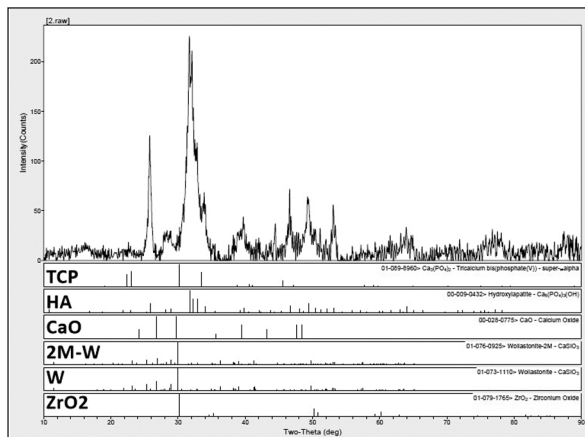
GRAPH 3: a) 2, b) 7, c) 14, d) 21-day EDS analysis of the H3W7 group samples kept in SBF.



GRAPH 4: a) 2, b) 7, c) 14, d) 21-day EDS analysis of the W group samples kept in SBF.



GRAPH 5: XRD figure of the HA group sample kept in the SBF for 21 days.



GRAPH 6: XRD figure of the H7W3 group sample kept in the SBF for 21 days.

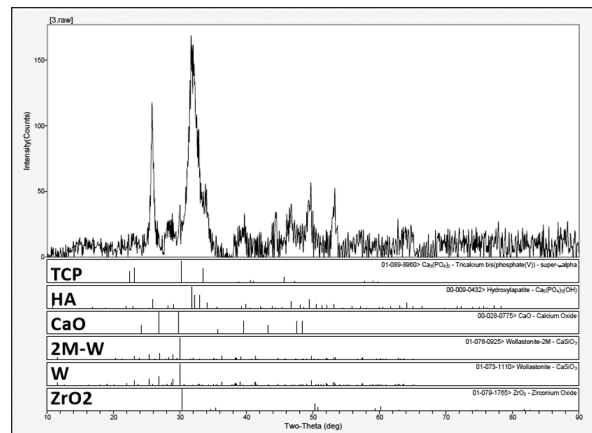
In the in-vivo study performed by Xue et al., Ti-6Al-4V alloy implants were coated with titanium and wollastonite using the plasma spray method to form two experimental groups.<sup>34</sup> More bone formation was reported at the end of one month compared to titanium-coated implants on the surface of wollastonite-coated implants placed in the cortical bone.

In studies examining the microstructure of coatings obtained by plasma spray method on titanium alloys, it was stated that wollastonite coatings were denser than HA coatings and had less porosity and micro-cracked lamella structure.<sup>9,11,16,35</sup> In our study, linear and continuous microcracks increased porosity and marked separation in the interface bond region were observed in the HA coating group

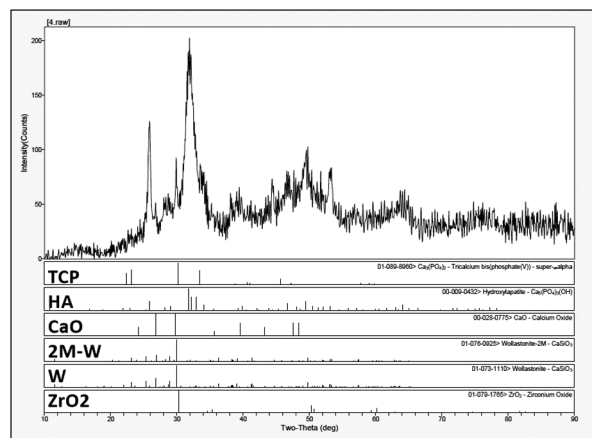
compared to the other groups. In the H7W3, H3W7 and W coating groups, a relatively less micro-crack and pore-containing lamella structure were observed. The mean binding values for H7W3 and H3W7 groups were significantly higher than the values of HA group, indicating that addition of wollastonite strengthens the coating structure.

In our SEM analysis where sample sections were examined, coating interface bond areas did not show any continuity in HA coatings. This result supports the low bonding values obtained from the HA coatings and shows similarity with many studies.<sup>10,13,29-31,36,37</sup> It is possible to mention a bonding continuity in the H7W3 group.

In our study, the bond strength values of the groups containing 100% wollastonite on zirconia ranged from 28 to 35 MPa.



GRAPH 7: XRD figure of the H3W7 group sample kept in the SBF for 21 days.



GRAPH 8: XRD figure of the W group sample kept in the SBF for 21 days.

The values we obtained were found to be lower than the pure wollastonite coating studies on titanium alloys even if they were similar.<sup>8,10,11,13,29,30,33,35</sup>

In a study conducted by Liu et al., Ti-6Al-4V alloys were coated with wollastonite/ TiO<sub>2</sub> powder mixtures prepared in different ratios with plasma spray method. The bond strength of the pure wollastonite coating was measured at around 40 MPa while the bond strength of the wollastonite/TiO<sub>2</sub> composite coatings was measured at around 30 MPa.<sup>13</sup>

In another study where wollastonite and zirconia powder mixtures and Ti-6Al-4V alloys were coated by the plasma spray method, the highest bond strength was measured in 100% wollastonite group.<sup>17</sup>

In similar studies examining bioactive calcium silicate ceramics and coatings, bond strength values of plasma spray coatings on Ti-6Al-4V alloys were found to be within a range of 39 - 42.8 MPa for pure wollastonite coatings and approximately 20 MPa bond value has been reported for pure HA coatings.<sup>10,35</sup>

In our study, in-vitro bioactivity of coated zirconia samples was tested in SBF for 2, 7, 14- and 21-day periods. These periods were determined based on the study of Liu et al. The SBF solution was prepared as described by Kokubo and Takadama. This method has been adopted as a standard by the International Organization for Standardization (ISO) to test in-vitro bioactive properties of materials.<sup>11,21,38</sup>

The formation of the CHA layer on the surface of the wollastonite in-vitro environment begins with the displacement of H<sup>+</sup> ions in the SBF with Ca<sup>2+</sup> ions on the coating surface. Subsequently, the SiO<sub>2</sub>-rich layer formed on the surface induces amorphous CaP precipitation. The CaP layer formed on the surface is crystallized into the CHA form over time, and it is a known fact that the layer of CHA accumulated on the surface becomes thicker as the duration increases.<sup>9,11,12,16,21</sup>

In all of the HA, H7W3, H3W7 and W sample groups which were kept in SBF, the formation of CHA starting with the precipitation of spherical particles on the coated surfaces and continuing with the growth of these particles was observed in the SEM images and confirmed by XRD analysis. Thickening

of the CHA layer was observed with the increase in incubation period. Our results show a similarity compared with the studies in this field.<sup>9-13,16,17,21,24,34,39-42</sup>

Liu et al. studied bioactivity of Ti-6Al-4V alloy samples in which calcium silicate was coated by plasma spray method. It was stated that CHA precipitation occurred within one hour on the sample surfaces kept in the SBF and the surface was completely covered with apatite layer within the first 24 hours in the bioactivity tests.<sup>9,11</sup>

In all of the HA, H7W3, H3W7 and W groups that we have carried out bioactivity test, forming of microcracks in the CHA layer was observed by SEM images. Researchers have observed the occurrence of micro-cracks in the coating and the CHA layer due to dehydration in the drying process. However, they have stated that these cracks could not be seen in-vivo applications since no dehydration in the body may be experienced.<sup>19,29</sup>

When the crack lines in the SEM images obtained from the sample surfaces were examined carefully; we have observed that uniform and spherical precipitation occurred during the experiment and microcracks were formed by dehydration of the apatite layer in the course of drying the samples extracted from the SBF. Irregular dislocations in spherical apatite deposits are consistent with the explanations of Gu et al. and Xie et al. Many studies that have performed bioactivity testing in this area have observed cracks similar to microcracks seen in our study.<sup>9-11,19,21,29,40,42,43</sup>

In the bioactivity study where wollastonite and zirconia powder mixtures and Ti-6Al-4V alloys were coated with plasma spray method, the CHA deposition was observed on all coating surfaces except for the ZrO<sub>2</sub> group and microcracks were seen in the CHA layer.<sup>39</sup>

In our EDS analysis, Ca and P ratios decreased over time in all groups. This reduction has been associated with the dissolution of coatings in SBF.<sup>9,11,12,16,34</sup> In the coatings containing wollastonite, the peaks of the silicium observed in the EDS analysis on the 2<sup>nd</sup> day can be associated with the "silicium-rich layer" formed by the silicium in the structure of wollastonite. The silicium-rich layer which remains in the deep layer with the thickening of the CHA layer

over time cannot be observed in EDS analysis on days 7, 14 and 21. Failure to monitor the peaks of silicon in studies has been associated with the presence of thickened CHA.<sup>9,11,12,34</sup>

## CONCLUSION

According to the results of our study, we suggest that the superior properties of zirconia and wollastonite can be combined on a single material. The results of our study where we conducted in-vitro analysis of the bond strengths and bioactive properties of zirconia samples coated with hydroxyapatite and wollastonite powders in different ratios are listed below:

Bond strength values measured between HA coating and zirconia were found to be significantly lower than H7W3, H3W7 and W groups.

The highest average bond strength belongs to the W group containing 100% wollastonite. However, there was no statistically significant difference between the bond strength values of H7W3, H3W7 and W groups containing wollastonite.

All of the hydroxyapatite and wollastonite coatings by plasma spray method on the zirconia samples

exhibited bioactive properties in simulated body fluid (SBF).

## Acknowledgements

The authors thank Dr. Caner Yılmaz and Dr. Turan Korkmaz.

## Source of Finance

During this study, no financial or spiritual support was received neither from any pharmaceutical company that has a direct connection with the research subject, nor from a company that provides or produces medical instruments and materials which may negatively affect the evaluation process of this study.

## Conflict of Interest

No conflicts of interest between the authors and / or family members of the scientific and medical committee members or members of the potential conflicts of interest, counseling, expertise, working conditions, share holding and similar situations in any firm.

## Authorship Contributions

**Idea/Concept:** Şefik Kolçakoğlu; **Design:** Şefik Kolçakoğlu; **Control/Supervision:** Fatih Üstel; **Data Collection and/or Processing:** Şefik Kolçakoğlu; **Analysis and/or Interpretation:** Fatih Üstel; **Literature Review:** Anıl Özyurt; **Writing the Article:** Anıl Özyurt; **Critical Review:** Anıl Özyurt; **References and Fundings:** Fatih Üstel.

## REFERENCES

- Piconi C, Maccauro G. Zirconia as a ceramic biomaterial. *Biomaterials*. 1999;20(1):1-25. [[Crossref](#)] [[PubMed](#)]
- Gahlert M, Röhling S, Wieland M, Eichhorn S, Küchenhoff H, Kniha H. A comparison study of the osseointegration of zirconia and titanium dental implants. A biomechanical evaluation in the maxilla of pigs. *Clin Implant Dent Relat Res*. 2010;12(4):297-305. [[Crossref](#)] [[PubMed](#)]
- Andriotelli M, Wenz HJ, Kohal RJ. Are ceramic implants a viable alternative to titanium implants? A systematic literature review. *Clin Oral Implants Res*. 2009;20(Suppl 4):32-47. [[Crossref](#)] [[PubMed](#)]
- Depprich R, Zipprich H, Ommerborn M, Naujoks C, Wiesmann HP, Kiattavorncharoen S, et al. Osseointegration of zirconia implants compared with titanium: an in vivo study. *Head Face Med*. 2008;4:30. [[Crossref](#)] [[PubMed](#)] [[PMC](#)]
- Langhoff JD, Voelter K, Scharnweber D, Schnabelrauch M, Schlottig F, Hefti T, et al. Comparison of chemically and pharmaceutically modified titanium and zirconia implant surfaces in dentistry: a study in sheep. *Int J Oral Maxillofac Surg*. 2008;37(12):1125-32. [[Crossref](#)] [[PubMed](#)]
- Sykaras N, Iacopino AM, Marker VA, Triplett RG, Woody RD. Implant materials, designs, and surface topographies: their effect on osseointegration. A literature review. *Int J Oral Maxillofac Implants*. 2000;15(5):675-90. [[PubMed](#)]
- Van Oirschot BAJA, Bronkhorst EM, van den Beucken JJJP, Meijer GJ, Jansen JA, Junker R. A systematic review on the long-term success of calcium phosphate plasma-sprayed dental implants. *Odontology*. 2016;104(3):347-56. [[Crossref](#)] [[PubMed](#)]
- Liu X. Novel bioactive ceramic coatings prepared by plasma spraying technology. *Biomed Pharmacother*. 2008;62(8):488. [[Crossref](#)]
- Liu X, Ding C, Wang Z. Apatite formed on the surface of plasma-sprayed wollastonite coating immersed in simulated body fluid. *Biomaterials*. 2001;22(14):2007-12. [[Crossref](#)] [[PubMed](#)]
- Liu X, Morra M, Carpi A, Li B. Bioactive calcium silicate ceramics and coatings. *Biomed Pharmacother*. 2008;62(8):526-9. [[Crossref](#)] [[PubMed](#)]
- Liu X, Tao S, Ding C. Bioactivity of plasma sprayed dicalcium silicate coatings. *Biomaterials*. 2002;23(3):963-8. [[Crossref](#)]
- Liu X, Ding C, Chu PK. Mechanism of apatite formation on wollastonite coatings in simulated body fluids. *Biomaterials*. 2004;25(10):1755-61. [[Crossref](#)] [[PubMed](#)]
- Liu X, Ding C. Plasma sprayed wollastonite/TiO<sub>2</sub> composite coatings on titanium alloys. *Biomaterials*. 2002;23(20):4065-77. [[Crossref](#)] [[PubMed](#)]
- Lee JK, Eum S, Kim J, Hwang KH. Fabrication of wollastonite coatings on zirconia by room temperature spray process. *J Nanosci Nanotechnol*. 2016;16(2):1996-9. [[Crossref](#)] [[PubMed](#)]



15. Chen Z, Zhai J, Wang D, Chen C. Bioactivity of hydroxyapatite/wollastonite composite films deposited by pulsed laser. *Ceramics International*. 2018;44(9):10204-9. [[Crossref](#)]
16. Magallanes-Perdomo M, Luklinska Z, De Aza A, Carrodegua R, De Aza S, Pena P. Bone-like forming ability of apatite-wollastonite glass ceramic. *J Eur Ceram Soc*. 2011;31:1549-61. [[Crossref](#)]
17. Liu X, Ding C. Bioactivity of plasma-sprayed wollastonite/ZrO<sub>2</sub> composite coating. *Surf Coat Technol*. 2003;172(2-3):270-8. [[Crossref](#)]
18. ASTM C. 633-01: Standard Test Method for Adhesion or Cohesion Strength of Thermal Spray Coatings. ASTM International, West Conshohocken, PA, USA. 2008. [[Link](#)]
19. Xie Y, Liu X, Zheng X, Ding C. Bioconductivity of plasma sprayed dicalcium silicate/titanium composite coatings on Ti-6Al-4V alloy. *Surf Coat Technol*. 2005;199(1):105-11. [[Crossref](#)]
20. Jemat A, Ghazali MJ, Razali M, Otsuka Y, Rajabi A. Effects of TiO<sub>2</sub> on microstructural, mechanical properties and in-vitro bioactivity of plasma sprayed yttria stabilised zirconia coatings for dental application. *Ceramics International*. 2018;44:4271-81. [[Crossref](#)]
21. Kokubo T, Takadama H. How useful is SBF in predicting in vivo bone bioactivity? *Biomaterials*. 2006;27(15):2907-15. [[Crossref](#)] [[PubMed](#)]
22. Verestiuc L, Morosanu C, Bercu M, Pasuk I, Mihailescu I. Chemical growth of calcium phosphate layers on magnetron sputtered HA films. *Journal of Crystal Growth*. 2004;264(1-3):483-91. [[Crossref](#)]
23. Garcia E, Maria Pm, Sainz MA. Thermally sprayed wollastonite and wollastonite-diopside compositions as new modulated bioactive coatings for metal implants. *Ceramics International*. 2018;44:12896-904. [[Crossref](#)]
24. Padmanabhan SK, Gervaso F, Carrozzo M, Scalera F, Sannino A, Licciulli A. Wollastonite/hydroxyapatite scaffolds with improved mechanical, bioactive and biodegradable properties for bone tissue engineering. *Ceramics International*. 2013;39:619-27. [[Crossref](#)]
25. Möller B, Terheyden H, Açil Y, Purcz NM, Hertrampf K, Tabakov A, et al. A comparison of biocompatibility and osseointegration of ceramic and titanium implants: an in vivo and in vitro study. *Int J Oral Maxillofac Surg*. 2012;41(5):638-45. [[Crossref](#)] [[PubMed](#)]
26. Delgado Ruíz RA, Calvo Guirado JL, Moreno P, Guardia J, Gomez Moreno G, Mate Sánchez J, et al. Femtosecond laser microstructuring of zirconia dental implants. *J Biomed Mater Res B Appl Biomater*. 2011;96(1):91-100. [[Crossref](#)] [[PubMed](#)]
27. Oliva J, Oliva X, Oliva JD. Five-year success rate of 831 consecutively placed zirconia dental implants in humans: a comparison of three different rough surfaces. *Int J Oral Maxillofac Implants*. 2010;25(2):336-44. [[PubMed](#)]
28. Özkurt Z, Kazazoğlu E. Zirconia dental implants: a literature review. *J Oral Implantol*. 2011;37(3):367-76. [[Crossref](#)] [[PubMed](#)]
29. Gu YW, Khor KA, Pan D, Cheang P. Activity of plasma sprayed yttria stabilized zirconia reinforced hydroxyapatite/Ti-6Al-4V composite coatings in simulated body fluid. *Biomaterials*. 2004;25(16):3177-85. [[Crossref](#)] [[PubMed](#)]
30. Zheng X, Huang M, Ding C. Bond strength of plasma-sprayed hydroxyapatite/Ti composite coatings. *Biomaterials*. 2000;21(8):841-9. [[Crossref](#)] [[PubMed](#)]
31. Chang E, Chang WJ, Wang BC, Yang C. Plasma spraying of zirconia-reinforced hydroxyapatite composite coatings on titanium: part I: phase, microstructure and bonding strength. *J Mater Sci Mater Med*. 1997;8(4):193-200. [[PubMed](#)]
32. Rodriguez HH, Vargas G, Cortés DA. Electrodeposition of bioactive wollastonite and porcelain-wollastonite coatings on 316L stainless steel. *Ceramics International*. 2008;34:1303-7. [[Crossref](#)]
33. Liang Y, Xie Y, Ji H, Huang L, Zheng X. Excellent stability of plasma-sprayed bioactive Ca<sub>3</sub>ZrSi<sub>2</sub>O<sub>9</sub> ceramic coating on Ti-6Al-4V. *Appl Surf Sci*. 2010;256(14):4677-81. [[Crossref](#)]
34. Xue W, Liu X, Zheng X, Ding C. In vivo evaluation of plasma-sprayed wollastonite coating. *Biomaterials*. 2005;26(17):3455-60. [[Crossref](#)] [[PubMed](#)]
35. Liu X, Ding C. Thermal properties and microstructure of a plasma sprayed wollastonite coating. *Journal of Thermal Spray Technology*. 2002;11:375-9. [[Crossref](#)]
36. Lamy D, Pierre AC, Heimann RB. Hydroxyapatite coatings with a bond coat of biomedical implants by plasma projection. *Journal of Materials Research*. 1996;11(3):681-6. [[Crossref](#)]
37. Darimont G, Cloots R, Heinen E, Seidel L, Legrand R. In vivo behaviour of hydroxyapatite coatings on titanium implants: a quantitative study in the rabbit. *Biomaterials*. 2002;23(12):2569-75. [[Crossref](#)] [[PubMed](#)]
38. Saber-Samandari S, Saber-Samandari S, Kiyazar S, Aghazadeh J, Sadeghi A. In vitro evaluation for apatite-forming ability of cellulose-based nanocomposite scaffolds for bone tissue engineering. *Int J Biol Macromol*. 2016;86:434-42. [[Crossref](#)] [[PubMed](#)]